

Total γN cross section in the energy range
 $\sqrt{s} = 40 - 250$ GeV

O. Lalakulich^{1,2}, Yu. Novoseltsev¹,
R. Novoseltseva¹, and G. Vereshkov^{1,2}

¹ Institute for Nuclear Research of Russian Academy of
Sciences, 117312 Moscow, Russia

² Research Institute of Physics, Rostov State University,
344090 Rostov-on-Don, Russia

Abstract

The results of measurements of γN total cross section, obtained by the method of photoproduction processes registration at the Baksan Underground Scintillation Telescope, are presented. These data at energies $\sqrt{s} = 40 - 130$ GeV confirm the effect of more rapid photon-hadron cross-section rise as compared to the hadron-hadron ones. It is shown, the increasing of the additive quark number in the products of photon hadronization can be one of the causes responsible for this effect. On the basis of the analysis of experimental data on both γN and $\gamma\gamma$ total cross sections, the status of direct and indirect cross-section measurements is discussed.

Keywords: photon-hadron interaction, cosmic ray muons

PACS: 13.60.-r, 13.40.Hb, 96.40.Tv

1 Introduction. Status of the data.

Since the first measurements from ZEUS [1] using 1995 data, information about the proton (nucleon) structure function F_2 at low Q^2 and γN cross section $\sigma_{\gamma N}(s)$ at high energies generates a lot of interest. In the energy range $\sqrt{s} = 100 \div 250$ GeV, the total cross section of γp interaction were determined by indirect method [2] on the basis of DESY data on proton structure functions [1]. At several points of energy scale around $\sqrt{s} = 200$ GeV, the cross section was measured by direct method — by photoproduction processes registration [3, 4]. The results obtained testify to more rapid photon–hadron cross section rise in comparison with the hadron–hadron ones. The physical nature of this more rapid rise is the main problem of γN physics, which is discussed in many papers. Modern interpretation in the framework of a Regge parametrization is done in [5]. The reviews of experimental data and theoretical approaches are given in [6, 7].

In this paper we present the results of measurements of $\sigma_{\gamma N}(s)$ in the region $\sqrt{s} = 40 \div 130$ GeV obtained at the Baksan Underground Scintillation Telescope (BUST) of Baksan Neutrino Observatory. In this experiment the hadronic and electromagnetic cascades produced by cosmic ray muons are registered. The BUST is situated at an effective depth of 8.5×10^4 g/cm² underground [8]. So only muons (with energy $E_\mu > 220$ GeV) and neutrinos can reach the telescope. That is the experiment conditions correspond to the pure muon beam with the known energy spectrum. Preliminary results were presented earlier [9], however the data on cross section $\sigma_{\gamma N}(s)$ were not reported in [9]. The data obtained in this paper confirm the effect of more rapid rise of photon-hadron cross section.

The theoretical basis of how to find the γN cross section from the data on muon interaction with nuclei was developed in [10], [11]. It was shown in this Refs., that in BUST experiment the number of hadronic cascades is proportional to $\sigma_{\gamma N}(s)$.

To interpret the experimental data, we propose a phenomenological theory based on the Vector Dominance Model (VDM) and the Additive Quark

Model (AQM). In this theory the violation of photon–hadron scaling is parametrised by two effects: 1) the rise of hadronization probability; 2) the rise of hadronization product, which is due to vector resonances decay on pions. It is shown, the experimental data on γN cross section allows to find the measures of these effects and than to predict the $\gamma\gamma$ cross section with high enough accuracy.

Let us introduce a quantitative characteristic of the effect of the photon–hadron scaling violation. According to the VDM

$$\sigma_{\gamma p}(s) = \sum_V P_{\gamma \rightarrow V}(s) \sigma_{Vp}(s), \quad (1)$$

where $P_{\gamma \rightarrow V}(s)$ is the probability of photon conversion to a vector meson V ; $\sigma_{Vp}(s)$ is the total cross section of Vp interaction. Making use the AQM [12] and U(3) symmetry of meson-nucleon interactions gives

$$\sigma_{Vp}(s) = \frac{2}{3} \bar{\sigma}_{Np}(3s/2), \quad V = \rho, \omega, \phi. \quad (2)$$

This allows to separate in (1) the contributions of ρ , ω , ϕ mesons:

$$\sigma_{\gamma p}^{(0)}(s) = P_{\gamma \rightarrow \rho\omega\phi}(s) \frac{2}{3} \bar{\sigma}_{Np}(3s/2) \quad (3)$$

where

$$P_{\gamma \rightarrow \rho\omega\phi}(s) = \sum_{V=\rho,\omega,\phi} P_{\gamma \rightarrow V}(s), \quad \bar{\sigma}_{Np} = \frac{1}{4}(\sigma_{pp} + \sigma_{\bar{p}p} + \sigma_{np} + \sigma_{\bar{n}p}). \quad (4)$$

The argument in the right–handed part of Eq. (2) is multiplicatively transformed ($3s/2$ instead of s), because the energies of interacting quark pairs in Vp and Np systems are different. The photon hadronization probability $P_{\gamma \rightarrow \rho\omega\phi} \approx P_{\gamma \rightarrow \rho\omega\phi}^{(0)} = 1/250$ is known from the data on $\gamma \rightarrow V$ transitions on the mass shells of vector mesons. So ρ, ω, ϕ contributions (i.e. $\sigma_{\gamma p}^{(0)}(s)$ function) can be expressed only in terms of the data on cross sections of nucleon-proton interactions. The function $\sigma_{\gamma p}^{(0)}(s)$, by virtue the specifying it experimental data are independent and the physical sense is clear, is referred to as the calibration curve for the cross section of γp interaction. It is clear,

the deviation of measured $\sigma_{\gamma p}(s)$ from the calibration curve contains an additional information about photon hadronization, which is not contained in $\sigma_{\gamma p}^{(0)}(s)$.

For constructing the calibration curve in the energy region $\sqrt{s} = 5.93 \div 22.97$ GeV, we use data from [13, 14]. In the region $\sqrt{s} = 30.4 \div 62.7$ GeV, the data of [15, 16] on $\sigma_{pp}(s)$ and $\sigma_{\bar{p}p}(s)$ are used (it seems to be reasonable to assume, that at such energies $\sigma_{pp} = \sigma_{np}$, $\sigma_{\bar{p}p} = \sigma_{\bar{p}n}$ with a good accuracy); for energies $\sqrt{s} = 200, 546, 900, 1800$ GeV we use the $\bar{p}p$ data from [17, 18, 19, 20]. These data, subjected to the scale transformation $3s_{Np}/2 = s_{\gamma p} \equiv s$, are fitted by the calibration curve

$$\sigma_{\gamma p}^{(0)}(s) = C \ln^2 \frac{s}{s_0} + A \left(1 + \frac{\Lambda_{01}^2}{s + \Lambda_{02}^2}\right) \quad (5)$$

$$C = 0.57777 \mu\text{b}, \quad \sqrt{s_0} = 2.198 \text{ GeV}, \quad A = 95.65 \mu\text{b},$$

$$\Lambda_{01} = 2.774 \text{ GeV}, \quad \Lambda_{02} = 3.589 \text{ GeV}.$$

The data and the calibration curve mentioned above, and also various experimental points on $\sigma_{\gamma p}(s)$ (including those of BUST) and two variants of their fit, corresponding to the two variants of the high energy points choice, are presented in Fig.1. The upper solid line represents the cross section $\sigma_{\gamma p}(s)$ as if the photon hadronizes only in the strongly bound $\pi^+\pi^-$ system; physical bases for invoking of this curve are discussed in section 3.

One can see from Fig.1, at low energies the photon-proton cross section asymptotically approaches the calibration curve. This testifies, that considerations used at constructing the calibration curve adequately reflect the physics at these energies. Essential deviations from the calibration curve emerge at $\sqrt{s} > 8$ GeV. At $\sqrt{s} = 200$ GeV the deviation of the cross section obtained by the photoproduction (direct) method achieves 25%. That derived from the extrapolation [2] of ZEUS data [1] (indirect) is even larger. The BUST data, obtained by the photoproduction method, are combined and fitted with both direct and indirect measurements. The results are shown in Fig.1 as the dashed and dotted lines correspondingly.

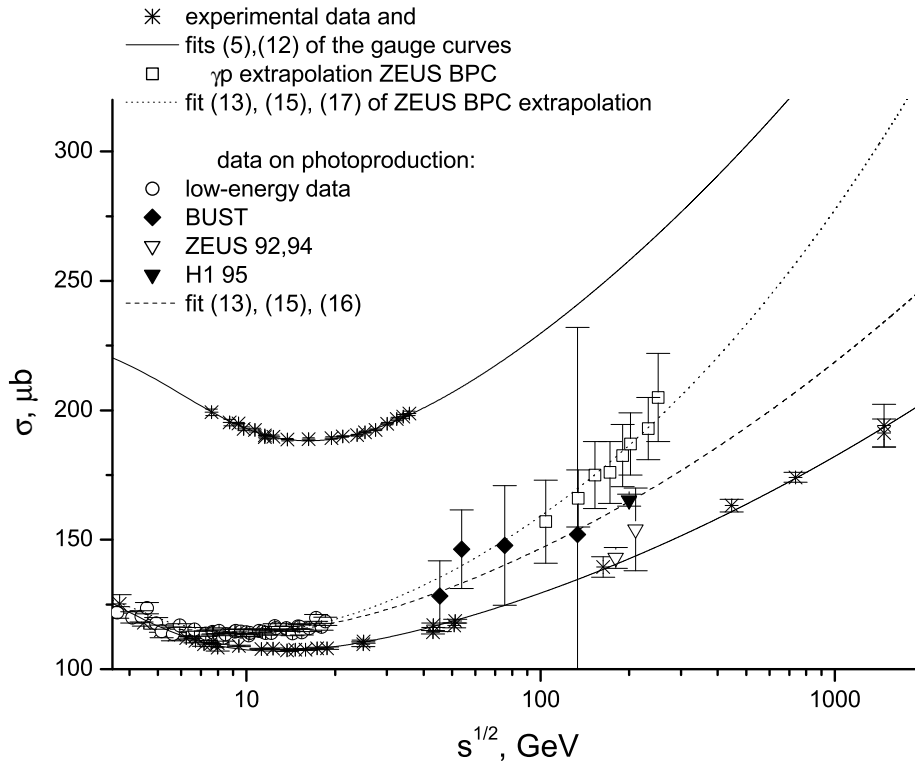


Figure 1: Calibration curves and cross section of γp interaction.

2 Experimental technique and the results at the BUST.

2.1 The measured variables.

In 1983 - 1989 at the BUST, the experiment on studying cross section $d\sigma_{\mu A}^{(h)}(E_\mu, E_c, q^2)/dE_c$ of inelastic scattering of Cosmic Ray (CR) muons on atomic nuclei was carried out [9, 21, 22]. Here $E_c = E_\mu - E'_\mu$ is the energy transferred from muon into the hadronic cascade, E_μ and E'_μ are muon ener-

gies in laboratory system before and after interaction. The average number of nucleons in the nuclei of the target was estimated as $\overline{A} = 26$. The events characterized by $E_c > 700$ GeV were selected.

The average value of the squared transferred four-momentum in our experiment, $-\overline{q^2} = \overline{Q^2} = 0.5 \text{ GeV}^2$, is much less than the characteristic squared energy in the centre-of-mass system of photon and nucleon, $s_{\gamma N} > (40 \text{ GeV})^2$ ($E_\gamma \geq 700$ GeV). This allows us to pose the problem on experimental measurements of interaction cross section $\sigma_{\gamma N}(s)$ of a real photon with a nucleon.

The problem of the measurement $\sigma_{\gamma N}$ in the processes with $\overline{Q^2} = 0.5 \text{ GeV}^2$ is nontrivial. In [10, 11] it was shown, that the differential cross section of inelastic μA scattering at small Q^2 can be represented as a product of $\sigma_{\gamma N}$ and a certain function. This function depends on Q^2 and other parameters taking into account the effects of shadowing in nuclei; its explicit form is given in the Refs. mentioned above. Notice, the factorization of $\sigma_{\gamma N}$ is a general property of μA cross section at small enough Q^2 ; the question is what is the particular value of Q^2 that the factorization can be actually performed at. In [10, 11] it is shown that this can be done if $Q^2 \leq 10 \text{ GeV}^2$. This structure of μA scattering cross section allows at $\overline{Q^2} \ll 10 \text{ GeV}^2$ to determine the $\sigma_{\gamma N}$ cross section, in spite of the fact that in each separate act of measurement the processes with $Q^2 \neq 0$ are fixed. In the expression for cross sections of inelastic μA scattering (at $E_c > 700$ GeV inelastic μA scattering initiates a hadronic cascade), it is possible to factorize the dependence from Q^2 , to integrate over this dependence and then to express the cross section directly through $\sigma_{\gamma N}(E_c)$ [11]:

$$\frac{d\sigma_{\mu A}^{(h)}(E_\mu, E_c)}{dE_c} = \frac{\alpha}{2\pi} \frac{AE_c}{E_\mu^2} \cdot \sigma_{\gamma N}(E_c) \cdot F_A(E_\mu, E_c), \quad (6)$$

where $F_A(E_\mu, E_c)$ is a function which takes into account shadowing of nucleons in a nucleus.

In our experiment $\overline{Q^2}$ is determined as

$$\overline{Q^2} = \frac{f_1(E_c)}{f_0(E_c)}, \quad f_n(E_c) = \int_{E_c}^{\infty} \frac{dN_\mu(E_\mu)}{dE_\mu} dE_\mu \int_{Q_{min}^2}^{Q_{max}^2} \frac{d^2\sigma(E_\mu, E_c, Q^2)}{dE_c dQ^2} \cdot Q^{2n} dQ^2, \quad n = 0, 1,$$

where $N_\mu(E_\mu)$ is the integral energy spectrum of CR muons (see Eq. (7)). At calculating the integral over Q^2 , we use the expression of $d^2\sigma(E_\mu, E_c, Q^2)/dE_c dQ^2$ and $\sigma_{\gamma N}(E_c)$ from [11] (this can be done because $\sigma_{\gamma N}(E_c)$ describes the experimental data fairly well) and restricted the integration range from Q_{min}^2 to 10 GeV². The contribution of the range $Q^2 > 10$ GeV² in $\overline{Q^2}$ value is $< 1\%$.

The integral energy spectrum of muons for zenith angles $\theta < 25^\circ$ was obtained in the special gauge experiment [22] and with an accuracy of 5% approximated by the expression:

$$N_\mu(> E; \theta, \phi) = k \cdot (E + E_H)^{-2.83}, \quad (7)$$

where $E_H = 230$ GeV, $k = const.$ At $\theta > 25^\circ$ we used the calculated muon spectrum obtained in Ref. [23, 24].

The BUST has sizes $16 \times 16 \times 11$ m³ and consists of four horizontal and four vertical scintillation planes [8]. In experiment [9, 21, 22] the four horizontal scintillation planes of the BUST together with the concrete layers between them were used as a calorimeter that registered electromagnetic and hadronic cascades generated by CR muons either in the rock immediately above the telescope ($\overline{A} = 25$) or in the matter of the telescope ($\overline{A} = 27$). Experimentally measured values are the differential spectra of energy deposition in the calorimeter from the electromagnetic ($j = e$) and hadronic ($j = h$) cascades

$$\frac{dN_j(\varepsilon)}{d\varepsilon} = \int \frac{\partial N_\mu(E_\mu; \theta, \phi)}{\partial E_\mu} \cdot \frac{d\sigma_{\mu A}^{(j)}(E_\mu, E_c)}{dE_c} \cdot n \cdot W(E_c, \varepsilon; \theta, \phi) S(\theta, \phi) dE_\mu dE_c \sin \theta d\theta d\phi. \quad (8)$$

Here ε is the sum of energy depositions in four horizontal scintillation layers of the BUST;

$\partial N_\mu(E_\mu; \theta, \phi)/\partial E_\mu$ is the differential spectrum of muons in a given direction at the BUST location;

$d\sigma_{\mu A}^{(j)}(E_\mu, E_c)/dE_c$ is the production cross section of electromagnetic or hadronic cascade with energy E_c by muon with energy E_μ ;

n is the number of nuclei in a unit volume of the detector (or of the rock);

$W(E_c, \varepsilon; \theta, \phi)$ is the probability of that a cascade of energy E_c deposits the energy ε in the telescope;

$S(\theta, \phi)$ is the area of the telescope in a direction θ, ϕ .

At calculating the probability $W(E_c, \varepsilon; \theta, \phi)$, electromagnetic and hadronic cascade curves, obtained by Monte Carlo simulation in view of real structure of the facility, are used. $W(E_c, \varepsilon; \theta, \phi)$ takes into account the integration over the thickness of the target, therefore only the integration over $S(\theta, \phi)$ remains in Eq. (8).

Muons produce cascades in the following processes:

- a) bremsstrahlung of photons,
- b) production of e^+e^- - pairs,
- c) production of high-energy knock-on electrons,
- d) inelastic scattering on nuclei.

The hadronic cascades are produced only in the process (d), the processes (a), (b), (c) produce the electromagnetic cascades. For the cross sections of the processes (a), (b), (c) the expressions were taken from Refs. [25, 26].

To obtain the cross section $\sigma_{\gamma N}(E_c)$ we use the ratio of numbers of hadronic and electromagnetic cascades

$$R(\Delta\varepsilon) = \frac{N_h(\Delta\varepsilon)}{N_e(\Delta\varepsilon)}, \quad (9)$$

having assumed the cross sections of electromagnetic processes are known. Making use of the ratio $R(\Delta\varepsilon)$ has an important advantage in comparison with the procedure of $\sigma_{\gamma N}$ determination directly from the data on hadronic cascades. The possible uncertainties in determination of $N_\mu(> E; \theta, \phi)$, $W(E_c, \varepsilon; \theta, \phi)$, $S(\theta, \phi)$ (see Eq.(8)) are nearly completely disappear in the ratio (9).

In an individual event we do not try to restore the cascade energy E_c on the energy deposition ε , because the error is equal to 30 – 60%. However, with a good enough accuracy of 2 – 3%, it is possible to calculate the average energies of electromagnetic and hadronic cascades creating the energy deposition in the facility in a given interval $\varepsilon_i \leq \varepsilon < \varepsilon_{i+1}$.

The properties of the BUST allow us to distinguish cascades generated on different muon trajectories (in the cases when the cascade is accompanied by a muon group), and two consecutive cascades on one and the same trajectory and, thus, to exclude errors in the determination of ε caused by these factors.

2.2 Separation of cascades.

To separate hadronic and electromagnetic cascades, we used the number of $\pi \rightarrow \mu \rightarrow e$ decays recorded in the event [9, 21]. In hadronic cascades the number of $\pi - \mu - e$ decays is 20-25 times more, than in electromagnetic ones. Recording the delayed pulse on the screen of 10-beams oscillograph is the feature of $\mu - e$ decay (each beam corresponds to the plane of the BUST). The separation procedure is based on the results of electromagnetic cascades modeling and consists in the following.

1) The probability $P(m, \varepsilon)$ of recording of m decays in the electromagnetic cascade, which creates the energy deposition ε in the facility, is calculated [21].

2) The separation criterion $m_0(\varepsilon)$ is determined, such that the probability χ of recording the number of decays $m > m_0(\varepsilon)$ in the electromagnetic cascade is $\leq 10^{-2}$,

$$\sum_{m=0}^{m_0} P(m; \varepsilon) = 1 - \chi(m_0, \varepsilon) \simeq 0.99. \quad (10)$$

3) Cascades with $m \leq m_0(\varepsilon)$ are considered as electromagnetic ones.

4) The calculated number of electromagnetic cascades with $m > m_0(\varepsilon)$ is subtracted from the number of cascades with $m > m_0(\varepsilon)$ (i.e. it is taken into account that the "tails" of distributions $P(m, \varepsilon)$ fall into the area $m > m_0(\varepsilon)$).

On the basis of (10) one can write

$$N(m \leq m_0(\varepsilon)) = N_e(\varepsilon) - N_e(\varepsilon) \cdot \chi(m_0, \varepsilon),$$

where $N_e(\varepsilon)$ is the actual number of electromagnetic cascades. Therefore the total number of electromagnetic cascades in the interval $\Delta\varepsilon$ is

$$N_e(\Delta\varepsilon) = \frac{N(m \leq m_0(\Delta\varepsilon))}{1 - \chi(m_0, \Delta\varepsilon)}.$$

The remaining cascades are considered as hadronic ones.

5) We do not take into account hadronic cascades falling into the area of electromagnetic ones. The calculations show, that the fraction of hadronic cascades with $m \leq m_0(\varepsilon)$ does not exceed 3 %. It is much less than the statistical error, which is estimated as $\sqrt{N_h}$.

Thus, the efficiency of the electromagnetic cascades separation from the hadronic ones is $\geq 99\%$; in this case the efficiency of separation of hadronic cascades from electromagnetic ones is $\simeq 97\%$.

2.3 The results of measurements.

In Table 1 the data are presented on the numbers of electromagnetic $N_e(\Delta\varepsilon)$ and hadronic $N_h(\Delta\varepsilon)$ cascades recorded in various intervals of energy deposition in the facility $\Delta\varepsilon = \varepsilon_{min} \div \varepsilon_{max}$. The last interval of $\Delta\varepsilon$ is not limited from the above: $\varepsilon > 573 \text{ GeV}$. The spectra are nonmonotone, because at small ε the observation time was smaller (the total time was $T_{rec} = 31650$ hours).

The average energy $\overline{E}_c^{(h)}$ of hadronic cascades, creating energy deposition in an interval $\varepsilon_{min} \leq \varepsilon < \varepsilon_{max}$, is identified with the energy of photon, $\overline{E}_\gamma \equiv \overline{E}_c^{(h)}$. For a given $\Delta\varepsilon$, the photon energy interval $E_{\gamma(min)} \div E_{\gamma(max)}$ is calculated. The last two columns of Table 1 comprise the photon–proton energies in the centre–of–mass system and the corresponding total cross sections; energies being given in GeV, cross sections being given in μb .

The information about $\sigma_{\gamma N}(s)$ is extracted from the ratio of numbers of hadronic and electromagnetic cascades, as it has mentioned in section 2.1 (Eq. (9)). The final results for $\sigma_{\gamma N}(E_\gamma)$ are obtained by integration of photon–nucleon interaction cross section over the energy interval $\Delta E_\gamma = f(\Delta\varepsilon)$ in

Table 1: The data on cascades and cross sections of γN interaction

ε_{min}	ε_{max}	$N_e(\Delta\varepsilon)$	$N_h(\Delta\varepsilon)$	$E_{\gamma(min)}$	$E_{\gamma(max)}$	$\overline{E_\gamma}$	\sqrt{s}	$\sigma_{\gamma N}$
77	133	1050	96	744	1260	1100	45.4	128 ± 14
133	230	1006	102	1260	2100	1550	53.9	146 ± 15
230	573	445	45	2100	4980	3030	75.4	148 ± 23
573		36	4	4980		9500	133.5	152 ± 80

view of the cross section dependence on energy. For this purpose the forecast of $\sigma_{\gamma N}(E_\gamma)$ offered in [11] and consecutively refining fit of experimental data are used, on which the calculated value $R_{cal}(\Delta\varepsilon_i)$ is determined. The deviation of experimental value $R_{exp}(\Delta\varepsilon_i)$ from the calculated one determines the deviation of actually measured cross section from the forecast.

Now we can compare the method of $\sigma_{\gamma N}$ measurements used in this experiment with those used in DESY experiments.

1. Direct method [3, 4] is based on photoproduction registration. The photon being on-mass-shell (the virtuality is negligible) is ensured by strict selection of the final hadronic states.

2. In the indirect method [1, 2] electron in the inclusive process $ep \rightarrow e+X$ is registered at small Q^2 ; the value of $\sigma_{\gamma N}$ is obtained by model-dependent extrapolation of the structure functions to $Q^2 = 0$.

3. In the method described in this paper the photoproduction of slightly virtual photon is registered. Since the cross section falls down rapidly at increasing Q^2 , the absolute majority of the events occur at very low Q^2 , $\overline{Q^2} = 0.5 \text{ GeV}^2$. At such small Q^2 , the cross section $\sigma_{\gamma N}$ is theoretically proved to be a multiplier at inelastic μA scattering cross section (Eq. (6)).

3 About possible physical reasons of rise of γN interaction cross section.

Two problems arise on a way to reduce photon–hadron interactions to hadron–hadron ones. The first problem concerns the initial hadronic states. In γp interaction these states are a proton with the known quark–gluon structure and a quark bag, created by a photon. The structure of the latter is unknown and, moreover, statistical by its nature. In the framework of the AQM the problem is formulated as follows: what number of additive quarks describes the quark bag created by the photon? This question naturally arises, when one takes into account big widths of vector resonances. At transition of a photon into ρ –meson, two alternative situations are possible: either ρ –meson is considered as an initial hadronic state and interacts with the proton as a single particle, or the initial state is the strongly bound $\pi^+\pi^-$ system having originated in the decay of ρ –meson [10]. One of the possible representations of this $\pi^+\pi^-$ system is a bag consisting of four additive quarks. In more general case the average number of additive quark–antiquark pairs must be considered as a function of energy of γp interaction.

The second problem is the dependence of photon hadronization probability $P_{\gamma \rightarrow V}(s)$ on the energy. At $\sqrt{s} > 10$ GeV it can be higher than the standard value 1/250 on 10–20%, for example, due to the nondiagonal transitions $\gamma \rightarrow V^* \rightarrow V$, where V^* is a highly–excited resonance, V is a basic vector state ($V = \rho, \omega, \phi \dots$) [10].

Let us turn to the phenomenological model that takes into account the above mentioned effects. Assume, that formation of the strongly bound $\pi^+\pi^-$ system in the act of $\gamma \rightarrow V \rightarrow 2\pi$ transition and its subsequent interaction with the proton is described by the model of four additive quarks. In this model the cross section of $2\pi p$ interaction is estimated by the formula

$$\sigma_{2\pi p}(s) = 2\bar{\sigma}_{\pi p}(s/2) \quad \bar{\sigma}_{\pi p} = \frac{1}{2}(\sigma_{\pi^+ p} + \sigma_{\pi^- p}).$$

Let $P_{V \rightarrow 2\pi}(s)$ be the probability of conversion of a vector meson V into 2π –

system before interaction of V with the proton. Then the cross section of γp interaction can be written as

$$\begin{aligned}\sigma_{\gamma p}(s) &= \sum_V P_{\gamma \rightarrow V}(s) (1 - P_{V \rightarrow 2\pi}(s)) \sigma_{Vp}(s) + \sum_V P_{\gamma \rightarrow V}(s) P_{V \rightarrow 2\pi}(s) \sigma_{2\pi p}(s) \\ &= \frac{2}{3} \sum_V P_{\gamma \rightarrow V}(s) (1 - P_{V \rightarrow 2\pi}(s)) \bar{\sigma}_{Np}(3s/2) + 2 \sum_V P_{\gamma \rightarrow V}(s) P_{V \rightarrow 2\pi}(s) \bar{\sigma}_{\pi p}(s/2)\end{aligned}\quad (11)$$

Formally substituting in (11) $\sum_V P_{\gamma \rightarrow V} = P_{\gamma \rightarrow V}^{(0)} = 1/250$, $P_{V \rightarrow 2\pi} = 1$, we obtain the so called conditional calibration curve

$$\sigma_{\gamma p}^{(1)}(s) = 2P_{\gamma \rightarrow V}^{(0)} \bar{\sigma}_{\pi p}(s/2)$$

For its constructing we use data of groups [13, 14]. The fit of these data has resulted in the following expression

$$\sigma_{\gamma p}^{(1)} = C_1 \ln^2 \frac{s}{s_1} + A_1 \left(1 + \frac{\Lambda_{11}^2}{s + \Lambda_{12}^2} \right) \quad (12)$$

$$C_1 = 1.155 \mu\text{b}, \quad \sqrt{s_1} = 1.672 \text{ GeV}, \quad A_1 = 152.0 \mu\text{b},$$

$$\Lambda_{11} = 5.006 \text{ GeV}, \quad \Lambda_{12} = 6.658 \text{ GeV}.$$

Due to the universality of the Froissart asymptotic of hadronic cross sections, the parameter $C_1 = 2C$ is fixed by combinatorial reasons. In Fig.1 the curve (12) is represented by the upper solid line.

Rewriting (11) in terms of calibration curves reads

$$\sigma_{\gamma p}(s) = k(s) \left[\left(1 - \bar{P}_{V \rightarrow 2\pi}(s) \right) \sigma_{\gamma p}^{(0)}(s) + \bar{P}_{V \rightarrow 2\pi}(s) \sigma_{\gamma p}^{(1)}(s) \right], \quad (13)$$

where

$$k(s) = 1 + \frac{1}{P_{\gamma \rightarrow V}^{(0)}} \sum_{V, V^*} \Delta P_{\gamma \rightarrow V^* \rightarrow V}(s), \quad (14)$$

$$\Delta P_{\gamma \rightarrow V^* \rightarrow V}(s) = \sum_{V, V^*} P_{\gamma \rightarrow V^* \rightarrow V}(s) - P_{\gamma \rightarrow V}^{(0)}, \quad P_{\gamma \rightarrow V}^{(0)} \simeq \sum_{V=\rho, \omega, \phi} P_{\gamma \rightarrow V}(s)$$

(see Eqs. (3), (4)).

The function $k(s)$ takes into account the rise of photon hadronization probability due to nondiagonal transitions; $\overline{P}_{V \rightarrow 2\pi}$ is the pionization probability averaged over all vector mesons.

One can easily see from Fig.1, that all measured cross sections of γp interactions lie between the two calibration curves. This allows to assume, that the data can be interpreted within the framework of a hypothesis about the certain dependence of the pionization probability on energy or, what is the same, of the emergency probability quark bag consisting of four additive quarks.

If we neglect all other factors increasing a photon hadronization probability (in particular, the nondiagonal transitions) and put in (13) $k(s) = 1$, then the probability $\overline{P}_{V \rightarrow 2\pi}(s)$ can be expressed only through the experimental data:

$$\overline{P}_{V \rightarrow 2\pi}(s) = \frac{\sigma_{\gamma p} - \sigma_{\gamma p}^{(0)}}{\sigma_{\gamma p}^{(1)} - \sigma_{\gamma p}^{(0)}}$$

The values, extracted in such way and their fits by the formula

$$\overline{P}_{V \rightarrow 2\pi}(s) = w \ln^n \frac{s}{s_2} \tag{15}$$

are shown in Fig. 2.

The first fit,

$$w = 0.0712, \sqrt{s_2} = 5.465 \text{ GeV}, n = 1/2 \quad \text{— for direct measurements;} \tag{16}$$

represented by the dashed line, is based on the BUST data and the direct data [3, 4]. The second fit,

$$w = 0.0140, \sqrt{s_2} = 2.166 \text{ GeV}, n = 3/2 \quad \text{— for indirect data;} \tag{17}$$

based on the BUST data and the indirect data [2], is shown by the dotted line.

Substituting (15) in (13), one derives the two curves for $\sigma_{\gamma p}(s)$ fitting the two sets of experimental data mentioned above, which are presented in Fig. 1.

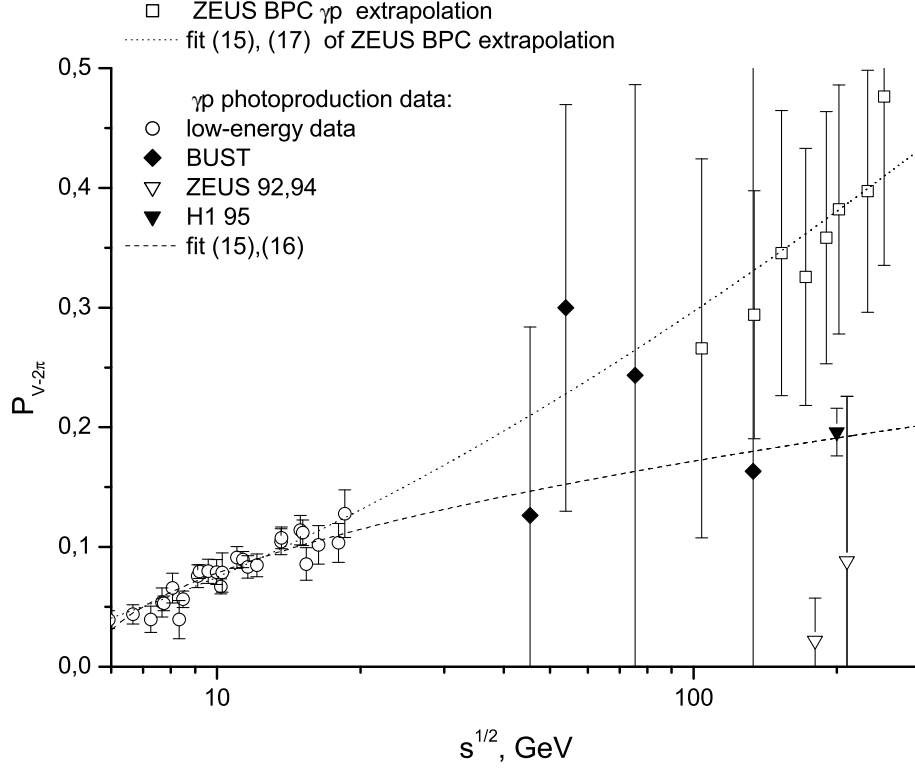


Figure 2: Probability of vector meson pionization in γp interaction.

The results obtained, in our opinion, testify that the average number of additive quarks in the products of photon hadronization monotonously increases with energy under the law

$$\bar{n}_{\gamma \rightarrow h}(s) = 2 \left(1 + w \ln^n \frac{s}{s_2} \right)$$

To obtain additional information, let us turn to the results of modeling of $\gamma\gamma$ interaction cross section on the basis of the γp one.

4 Modeling of $\gamma\gamma$ interaction cross section and its comparison with the experimental data.

The cross section of $\gamma\gamma$ interaction is expressed through the same probabilities of photon hadronization and cross sections of hadronic interactions, which appear in the model of γp interactions in Section 3. The first step of the theoretical cross section calculation is obvious:

$$\begin{aligned} \sigma_{\gamma\gamma}(s) = k^2(s) \left(P_{\gamma \rightarrow V}^{(0)} \right)^2 & \left[\left(1 - \bar{P}_{V \rightarrow 2\pi}(s) \right)^2 \sigma_{VV}(s) \right. \\ & \left. + 2\bar{P}_{V \rightarrow 2\pi}(s) \left(1 - \bar{P}_{V \rightarrow 2\pi}(s) \right) \sigma_{2\pi V}(s) + \bar{P}_{V \rightarrow 2\pi}^2(s) \sigma_{2\pi 2\pi}(s) \right]. \end{aligned} \quad (18)$$

Further on we express the cross sections of meson and two-pion interactions through the experimentally measured ones, simultaneously performing (according to the AQM) the scale transformation of arguments:

$$\begin{aligned} \sigma_{\gamma\gamma}(s) = k^2(s) \left(P_{\gamma \rightarrow V}^{(0)} \right)^2 & \left[\left(1 - \bar{P}_{V \rightarrow 2\pi}(s) \right)^2 \cdot \frac{4}{9} \sigma_{Np}(9s/4) \right. \\ & \left. + 2\bar{P}_{V \rightarrow 2\pi}(s) \left(1 - \bar{P}_{V \rightarrow 2\pi}(s) \right) \cdot \frac{4}{3} \sigma_{\pi p}(3s/4) + \bar{P}_{V \rightarrow 2\pi}^2(s) \cdot 4 \frac{\sigma_{\pi\pi}^2(3s/8)}{\sigma_{Np}(9s/16)} \right]. \end{aligned} \quad (19)$$

At obtaining (19) we use one more relation of the AQM: $\sigma_{\pi\pi}(s) = \sigma_{\pi p}^2(3s/2)/\sigma_{Np}(9s/4)$. The final result is convenient to present via the calibration curves:

$$\begin{aligned} \sigma_{\gamma\gamma}(s) = k^2(s) \cdot \frac{1}{250} \cdot \frac{2}{3} & \left[\left(1 - \bar{P}_{V \rightarrow 2\pi}(s) \right)^2 \cdot \sigma_{\gamma p}^{(0)}(3s/2) \right. \\ & \left. + 2\bar{P}_{V \rightarrow 2\pi}(s) \left(1 - \bar{P}_{V \rightarrow 2\pi}(s) \right) \cdot \sigma_{\gamma p}^{(1)}(3s/2) + \bar{P}_{V \rightarrow 2\pi}^2(s) \cdot \frac{\left(\sigma_{\gamma p}^{(1)}(3s/4) \right)^2}{\sigma_{\gamma p}^{(0)}(3s/8)} \right]. \end{aligned} \quad (20)$$

In Fig. 3 the experimental data on $\sigma_{\gamma\gamma}(s)$ cross section from [27] and the theoretical predictions (20) at $k(s) = 1$ for two variants of photon hadronization probability (16) and (17) are shown.

The experimental uncertainties for this reaction, as well as those for γp one, do not allow to fix unambiguously the variant of high-energy behaviour

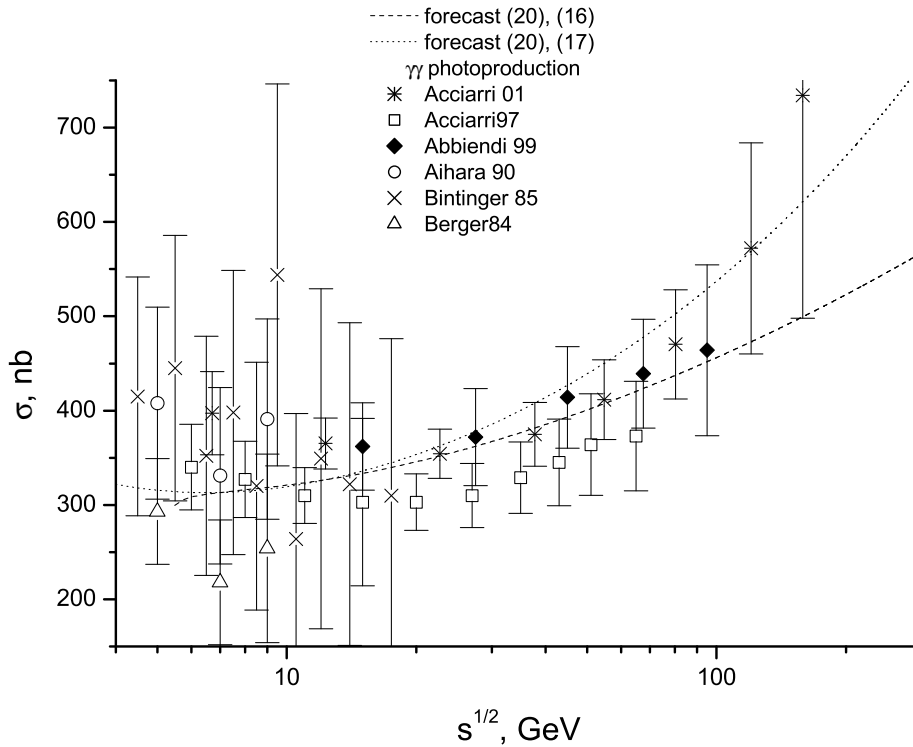


Figure 3: Cross section of $\gamma\gamma$ interaction and its modeling.

of $\sigma_{\gamma p}(s)$ and $\sigma_{\gamma\gamma}(s)$. However, the data on $\sigma_{\gamma\gamma}(s)$ at $\sqrt{s} < 100 \text{ GeV}$, which have rather small errors, agree better with the forecast made on the basis of direct measurements of γp cross sections.

We would like to thank Dr. V. Bakatanov for the help in carrying out the experiment, Prof. L. Bezrukov, Prof. S. Mikheyev and Dr. A. Butkevich for the helpful discussions. This work is supported by the Federal Program "Integration", Grant No. E0157.

References

- [1] ZEUS Collaboration, J. Breitweg *et al.*, Phys. Lett. B **407**, 432 (1997); Preprint DESY-00-071.
- [2] ZEUS Collaboration, Contribution to the International Europhysics Conference on High Energy Physics'99, Tampere, 15-23 July 1999.
- [3] ZEUS Collaboration, M. Derrick *et al.*, Phys. Lett. B **293**, 465 (1992); Z. Phys. C **63**, 391 (1994). ZEUS Collaboration, S. Chekanov *et al.*, Nucl. Phys. B**627**, 3 (2002).
- [4] H1 Collaboration, S. Aid *et al.*, Z. Phys. C **69**, 27 (1995).
- [5] A. Donnachie, P. V. Landshoff, Phys. Lett. B**518**, 63 (2001).
- [6] Ch. Amelung (for ZEUS and H1 Collaborations), BONN-HE-99-06, Contributed to the proceedings of International Conference and 8th Blois Workshop on Elastic and Diffractive Scattering (EDS 99), Protvino, Russia, 27 Jun - 2 Jul 1999. (hep-ex/9911005)
- [7] R. M. Godbole, G. Pancheri, Nucl. Instrum. Meth. A**472**, 205 (2001).
- [8] E.N. Alexeyev *et al.*, in Proc. XVI ICRC, Kyoto, 1979, v.10, p.276.
- [9] V.N. Bakatanov, Yu.F. Novoseltsev *et al.* Sov.J. Letters in JETP. **48**, 129 (1988);
- [10] L.B. Bezrukov, E.V. Bugaev, Sov.J. Yad. Phys. **32**, 1636 (1980);
- [11] L.B. Bezrukov, E.V. Bugaev, Sov.J. Yad. Phys. **33**, 1195 (1981).
- [12] V.V. Anisovich, M.N. Kobrinsky, Yu. Niri, Yu.M. Shabelsky, Sov.J. Uspekhi Fizicheskikh Nauk **144**, 553 (1984).
- [13] S.P. Denisov *et al.*, Phys. Lett. B **36**, 415 (1971); Nucl. Phys. B **65**, 1 (1973).
- [14] A.S. Carrol *et al.*, Phys. Lett. B **61**, 303 (1976); Phys. Lett. B **80**, 423 (1979).

- [15] N. Amos *et al.*, Nucl. Phys. B **262**, 689 (1985).
- [16] G. Carboni *et al.*, Nucl. Phys. B **254**, 697 (1985).
- [17] G. Arnison *et al.*, Phys. Lett. B **128**, 336 (1983).
- [18] F. Abe *et al.*, Phys. Rev. D **50**, 5500 (1994).
- [19] G.J. Alner *et al.*, Z. Phys. C **32**, 153 (1986).
- [20] N. Amos *et al.*, Phys. Rev. Lett. **68**, 2433 (1992); C. Avila *et al.*, Phys. Lett. B **445**, 419 (1998).
- [21] Yu.F. Novoseltsev, Ph.D. Thesis, INR of Academy of Sciences of USSR, Moscow, 1988.
- [22] V.N. Bakatanov, Yu.F. Novoseltsev *et al.* Sov.J. Yad. Phys. **55**, 2107 (1992); Sov. J. Nucl. Phys. **55**, 1169 (1992).
- [23] V.I. Gurentsov, Institute for Nuclear Research preprint, P-0379, Moscow, (1984).
- [24] V.I. Gurentsov, G.T. Zatsepin, E.D. Mihal'chi, Sov.J. Yad. Phys. **23**, 1001 (1976).
- [25] E.V. Bugaev, Yu.D. Kotov, I.L. Rozental, Cosmic muons and neutrino (Atomizdat, Moscow, 1970)
- [26] L.B. Bezrukov, E.V. Bugaev, in Proc. 17 ICRC, Paris, 1981, v.7, p.102.
- [27] D.E. Groom *et al.* (Particle Data Group) Eur. Phys. Jour. C **15**, 1 (2000).